THE IONOSPHERIC TOTAL ELECTRON CONTENT RESPONSE TO THE 17TH -18TH MARCH 2015 GEOMAGNETIC STROM OVER THE ARCTIC REGION

Abstract

The commencement of the "St. Patrick's day geomagnetic storm" on March 17th, 2015 led to multiple fluctuations in electron density within the ionosphere, resulting in significant disruptions in Total Electron Content at high latitudes in the northern hemisphere. Through the utilization of ground-based Global Navigation Satellite Systems (GNSS) receivers, we examined the ionospheric reaction to the primary phase of the most severe storm in the current solar cycle, focusing on the Total Electron Content observed in the Arctic regions. This research delves into the ionospheric behavior during the geomagnetic storm that occurred on March 17-18, 2015, which stood out as the most intense event in the 24th solar cycle. Total Electron Content data was gathered from three stations - Cambridge Bay(69.101929 N, 254.884829 E), Eureka (79.990089 N , 274.097557 E), and Rabbit Lake (58.226935 N, 256.322945 E) - utilizing Global Positioning System (GPS) receivers from the Canadian High Arctic Ionospheric Network (CHAIN). Our analysis revealed a notably lower TEC reading in Cambridge Bay compared to Eureka and Rabbit Lake during the storm period.

Keywords: geomagnetic storm, electron content, Arctic regions, magnetosphere

Introduction:

Temporary disruptions in Earth's magnetosphere are called geomagnetic storms. A geomagnetic storm is caused by a solar particle stream that impacts the Earth's magnetosphere through a coronal mass ejection (CME) or corotating interaction region. (Gonzalez et al. 1994, 1999; Moldwin 2008) CMEs can be visualized as bright structures that radiate from the solar corona with velocities between 10 km/s and 2000 km/s (Hundhausen 1999). The CME emits a large amount of plasma from its corona. The CIR is a long-lived, large-scale plasma structure (Heber et al. 1999) that is generated in the low and mid-latitude regions of the heliosphere by the interaction of a stable fast solar wind flow and the surrounding slow solar wind (Heber et al. 1999). During geomagnetic storms, the behavior of the ionosphere can change, resulting in an increase or decrease in plasma density (Rishbeth 1963; McNamara 1991; Moldwin 2008). The increase or decrease in plasma density is called a positive or negative ionospheric storm (Rishbeth 1963; Danilov and Morozova 1985; Schunk and Sojka 1996; Balan et al. 2013; Horvath and Lovell 2015; Matamba et al. 2015). The ionosphere responds differently to specific geomagnetic storms based on the timing of sudden storm outbreaks (SSCs), the season, solar activity, and the latitudinal region in which the ionosphere is located (Prölss 1995; Gao et al. 2008; Vijaya Lekshmi et al. 2011). During geomagnetic storms, the ionosphere is highly volatile,

which affects radio frequency (RF) radio communications. When solar radiation events occur, 4,444 X-rays are directed at the Earth, knocking 4,444 electrons out of atoms in the ionosphere, resulting in an unusually high density of free electrons in the lower ionosphere. High free electron densities (also called sudden ionospheric disturbances) absorb HF radio waves, resulting in disturbances in RF communications and trans-electronic layer global navigation satellite systems. Vertical E × B drift is one of the parameters that influences ionospheric variations, contributing to storm effects and Rayleigh-Taylor instability, especially near the equator and at low latitudes (Sekar and Raghavarao 1987). When the plasma is lifted upwards to an altitude where the recombination rate is low, photoionization occurs in the lower ionosphere, creating a new plasma that replaces the plasma lifted (e.g., Kelley 1989). The vertical E × B drift is modified by the instantaneous penetrating electric field (PPEF) and neutral winds from storm-related activities. (Balan et al., 2009, 2010). Depending on the configuration of the PPEF, which moves eastward during the day and westward during the night, the direction and magnitude of the vertical E × B drift change, resulting in significant increases or decreases in plasma density, resulting in generation or It also affects the impact. Suppression can be affected by anomalies in the hours after sunset. During a strong eastward daytime PPEF event, the equatorial plasma fountain rapidly disintegrates due to the effects of equatorial neutral winds that affect plasma diffusion and because it lifts the ionosphere to higher altitudes, reducing the recombination rate. Developing into superfountains (Kelley et al., 2004; Balan et al. Therefore, the mechanical influence of equatorial neutral winds combined with PPEF events causes positive ionospheric storms (e.g., Werner et al., 1999; Lin et al., 2005; Gonzalez et al., 2005; Gesetz et al., 2008; Baran et al., 2009, 2010). Matamba et al. (2015); Liu et al. (2016); Dugassa et al. (2019). Another possible cause of positive ionospheric storms is moving atmospheric disturbances (TADs), which manifest as moving ionospheric disturbances (TIDs) (Ngwira et al. 2012; Amabayo et al. 2012). 2012; Information et al. (2013). On the other hand, the perturbed electric dynamo field (DDEF) is oriented to the west or east during the day or night and causes a decrease or increase in plasma density within the ionosphere depending on the prevailing conditions (Tsurutani et al., 2004; Fuller-Rowell, 2002). Furthermore, for geomagnetic storms over the geomagnetic equator, strong PPEF alone has only a negative effect on the ionospheric density (e.g., Balan et al., 2009, 2010). Negative effects on the ionosphere during geomagnetic storms may also be due to changes in neutral composition resulting from joule heating within the auroral ellipse, which reduces the thermosphere [O]/[N2] ratio in the F2 region. (e.g., Danilov and Morozova, 1985; Liu et al., 2016)., the equatorward movement of the electron density trough from high to low latitudes (e.g., Mendillo et al. 1974), and the enhancement of the fountain effect on the magnetic equator, the trough (region) reduces electron density. Magnetic equator (e.g., Zhao et al., 2005; Liu et al., 2010). Depending on the configuration of the PPEF, which moves eastward during the day and westward during the night, the direction and magnitude of the vertical E × B drift changes, resulting in significant increases or decreases in plasma density, resulting in generation or It also affects the impact. Suppression can be affected by anomalies in the hours after sunset. During strong eastward daytime PPEF events, the equatorial plasma

fountain affects plasma diffusion due to the effect of equatorial neutral winds to lift the ionosphere to higher altitudes while reducing the recombination rate. rapidly develops into superfountains (Kelley et al 2004; Balan) et al. Therefore, the mechanical influence of equatorial neutral winds combined with PPEF events can cause positive ionospheric storms (e.g. : Werner et al. 1999; Lin et al. 2005; Gonzalez et al. 2005; Gesetz et al. 2008; Baran et al. 2009, 2010. Matamba et al. 2015; Liu et al. 2016; Dugassa et al. 2019). Another possible cause of positive ionospheric storms is moving atmospheric disturbances (TADs), which manifest as moving ionospheric disturbances (TIDs) (Ngwira et al. 2012; Amabayo et al. 2012). 2012; Informationet al. 2013). On the other hand, the perturbed electric dynamo field (DDEF) is oriented to the west/east during the day/night and causes a decrease/increase in plasma density within the ionosphere depending on the prevailing conditions (Tsurutani et al. 2004; Fuller Rowell) . . other. (2002). Furthermore, for geomagnetic storms over the geomagnetic equator, strong PPEF alone has only a negative effect on the ionosphericdensity (e.g. Balan et al. 2009, 2010). Negative effects on the ionosphere during geomagnetic storms may also be due to changes in neutral composition resulting from Joule heating within the auroral ellipse, which reduces the thermosphere [O]/[N2] ratio in the F2 region. (e.g.Danilov and Morozova 1985). ;Liu et al. 2016), equatorward movement of mid-latitude electron density troughs from high to low latitudes (e.g. Mendillo et al. 1974), and enhancement of the fountain effect on the magnetic equator. (area) decreases in density along the magnetic equator) (e.g. Zhao et al. 2005; Liu et al. 2010). The extent of these ionospheric impacts generally relies upon the condition of the shifting ionosphere, its Total electron content (TEC) and the recurrence of electromagnetic waves. The unique changes of the ionosphere are most effectively separated into normal and abrupt ones. Standard changes are straightforwardly identified with the periodicity of the variables impacting them, like the sun powered cycle. These ordinary varieties are to some degree simple to display (Bilitza et al., 2008; Maruyama et al. 2009). The ionospheric storms (aggravations in the earthly ionosphere delivered by geomagnetic storms) cause huge unsettling influences for innovative frameworks, for example, the static or dynamical situating with GNSS satellites, and others, which rely upon the transionospheric correspondences. Essentially, in correlation with under calm conditions, the electron thickness can increment or diminishing during geomagnetic storm periods. These changes, which have been called positive ionospheric tempest or positive tempest impact and negative ionospheric tempest or negative tempest impact individually, happen in light of the fact that there is critical energy input (from the sun based breeze) into the polar ionosphere, for the most part over a time of a few hours to a day. A few driver powers have been utilized to clarify the ionospheric impacts during storms at various scopes. For instance, it is accepted that level convection overwhelms in the polar covers, and structure changes, molecule precipitation and electric fields rule in the auroral zones, while electric fields, meridional breezes and creation changes rule at tropical and low scopes In the auroral and polar ionosphere, those abnormalities at an alternate scale have a typical element during geomagnetic storms, which causes vacillations in the Total Electron Content (TEC). Thusly, the limited scale ionospheric plasma thickness inconsistencies produce quick change in the abundancy and period of

transionospheric radio signs, which is known as sparkle. The huge scope inconsistencies and related TEC vacillations an muddle stage vagueness goal, increment the quantity of uncorrected cycle slips and misfortunes of sign lock in GNSS. Since there are moderately inadequate outcomes for TEC.The large-scale irregularities and associated TEC fluctuations can complicate phase ambiguity resolution, increase the number of uncorrected cycle slips and losses of signal lock in GNSS. Because there are relatively sparse results for TEC at sub-auroral, auroral and polar latitudes in this paper we analyze the behavior of TEC at three stations located in the Arctic sectors during intense geomagnetic storms in the 2015(Nie et al, 2022)

.

Data and methodology

Figure 1 shows geomagnetic coordinates of the collocated CHAIN GPS receivers used in this study. CHAIN GPS receivers are GPS Ionospheric Scintillation and TEC Monitors (GISTMs) model GSV4000B (Van Dierendonck and Arbesser-Rastburg, 2004). A GISTM consists of a NovAtel OEM4 dual-frequency receiver with special firmware specifically configured to measure amplitude and phase scintillation derived from the L1 frequency GPS signals and ionospheric TEC derived from the L1 and L2 frequency GPS signals. This receiver is capable of tracking and reporting scintillation and TEC measurements from up to 10 GPS satellites in view. Phase and amplitude data are sampled and logged, either in raw form or detrended, at a rate of 50 Hz. Receivers are currently fed by a NovAtel GPS-702 antenna. Temporal resolution for TEC data in this study is 1 s. The spatial resolution of TEC measurements varies with the speed of the signal path through the ionosphere, which, in turn, varies with altitude of ionization and satellite elevation. For 1s TEC measurements and a satellite elevation cutoff of 25°, the spatial resolution is between 18 and 350 m. At most occasions, 8 to 10 GPS satellites are apparent to a solitary ground recipient. From GPS information we figure the complete electron content (TEC), a worth coordinated in a 1 m^2 section along the satellite to collector raypath. Detective is determined in TEC units (TECu), where 1 TECu = 1016 electrons for each square meter.

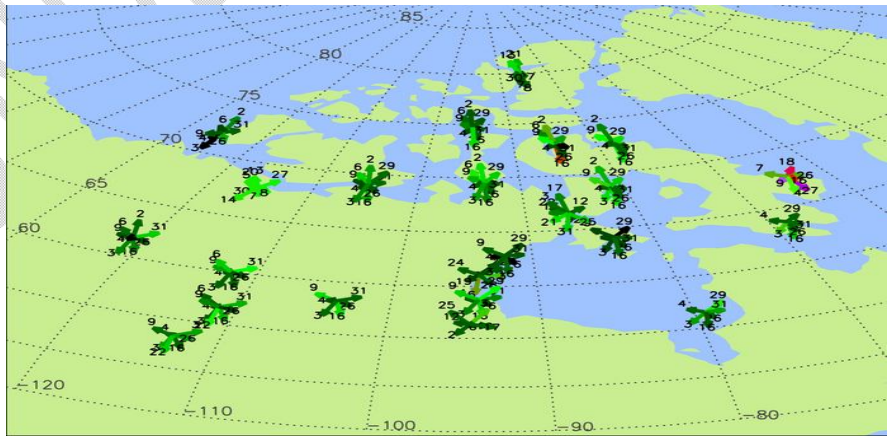

Figure 1: CHAIN Ionospheric Network over Arctic Region

Table 1. Geographic and Geomagnetic Coordinates of Stations Used in the Study

Name	Geo Lat	Geo Long	Instrument	Model
Cambridge Bay (CBB)	69.101929 N	254.884829 E	GISTM/GPS	GSV4004B
Eureka (EUR)	79.990089 N	274.097557 E	GISTM/GPS	GSV4004B
Rabbit Lake (RAB)	58.226935 N	256.322945 E	GISTM/GPS	PolaRxS

In this paper, we are researching subtlety the overall effect of the St. Patrick's Day tempests of March 2015 on the ionosphere over the northern polar cap locale. Exceptionally compelling are the positive ionospheric storms saw at the northern polar stations Cambridge Bay, Eureka and Rabbit Lake in the attractive tempests, which propose that the plasma thickness develops along these lines during comparable geophysical conditions. While the commitments of different tempest time wonders toward the arrangement of TOI during these tempests have been broadly contemplated, the job of outer driving instruments in altering the reaction of the polar ionosphere has not been focused. Consequently, the principle objective of the investigation is to break down exhaustively the systems that lead to the age of positive ionospheric storms over the northern polar cap area. In the accompanying, we depict our outcomes in subtleties and talk about their importance in creating comprehension of the reaction of the Earth's polar ionospheric framework to geomagnetic storms.

Result and Discussion

Observation of geomagnetic condition we are describing in figure 2.The severe geomagnetic storm occurred on 17 March 2015 and caused the dramatic response in the ionosphere–plasmasphere–magnetosphere system. Figure 1 shows the variations of interplanetary and geomagnetic parameters during 15–20 March 2015.

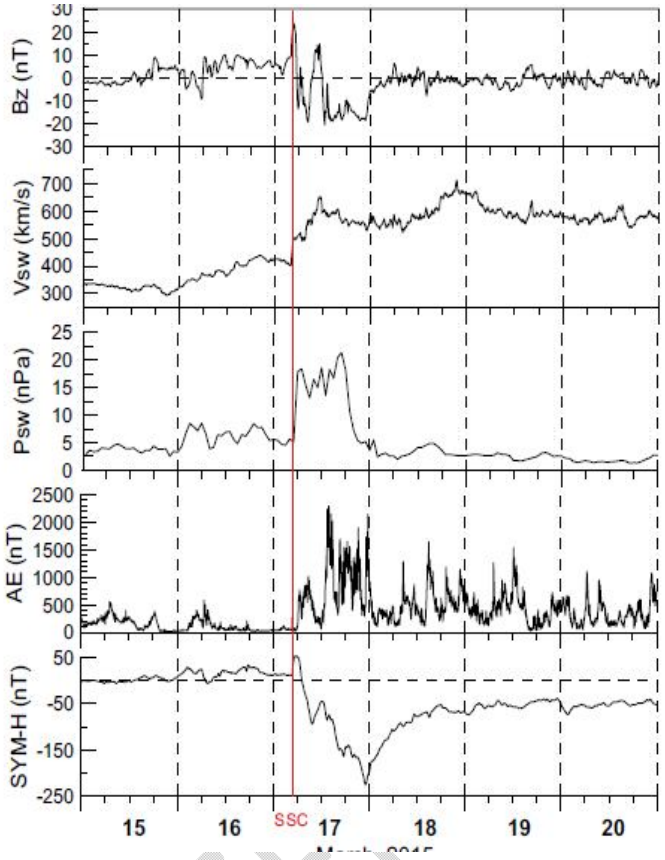

Fig 2.Observation of geomagnetic condition

The sudden storm commencement (SSC) was registered at ~0445 UT and then there was a quick drop of the SYM-H index to the value of −226 nT, observed at ~2300 UT, with a couple of local minima of −93 and −164 nT at ~0940 and ~1740 UT respectively (Fig. 1). The planetary index of the geomagnetic activity Kp reached the maximum value of 8 after ~12 UT on 17 March 2015, qualifying it as a severe geomagnetic storm.During the main phase of the storm (17 March), the interplanetary magnetic field (IMF) orientation displayed a highly complex behavior. Three IMF components (top panels of Fig. 1) switched several times from positive to negative values and vice versa. Right after the shock arrival, the northward IMF Bz component reached the value of about 25 nT. At ~0530 UT the IMF Bz turned southward and reached the first minimal value of −18 nT at 0615 UT. Then the IMF Bz sharply turned northward and varied significantly between north and south during ~8 h. After ~1340 UT the Bz turned southward again and remained south till the end of this day. From ~06 till 11 UT, there are observed dominating positive Bx and negative By with peak values of 16.5 and −16.8 nT for Bx and By, respectively. During 11–15 UT with the new southward turning of Bz, the opposite situation with Bx/By domination occurred—Bx became negative with the minimal values of −14 nT while By component became positive with the peak of 30 nT. After 15 UT, IMF By turned sharply to

negative values, reaching −8 nT, and then again to the positive ones with the new peak of 20 nT around 18 UT.Kamide and Kusano (2015) reported that this severe geomagnetic storm (G4 level) was a result from the superposition of two successive, moderate storms, driven by two successive, southward IMF structures. The intense geomagnetic storm on 17–18 March 2015 leads to the auroral particle precipitation and an enhancement of the substorm activity.

Response of the High latitude northern ionosphere

To understand the plasma density variations in the southern polar ionosphere during 17March 2015, we examined the variation of TEC at the Arctic stations, is shown in Figures 3 respectively

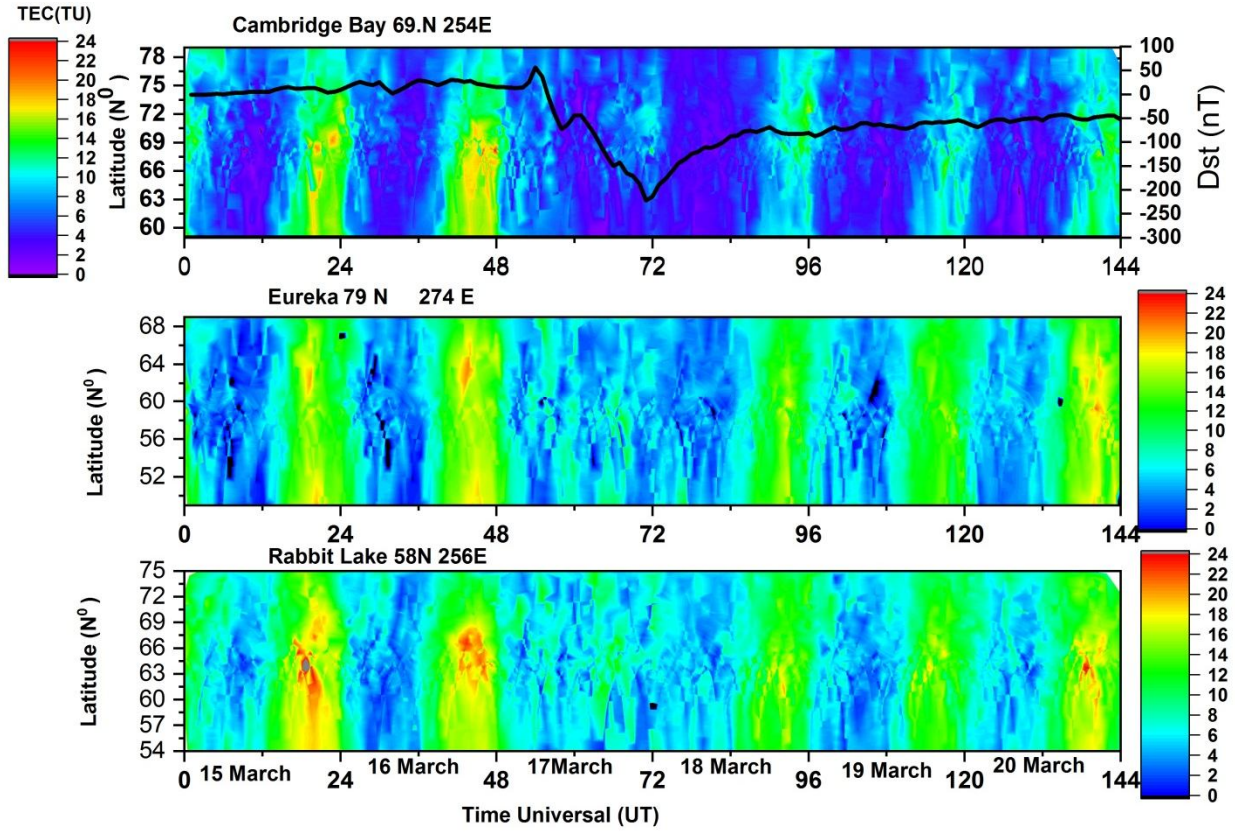

Figure 3. TEC variation over Arctic Region ionosphere during 15-20, March 2015

Figure 3 is composed of four panel including Dst fluctuation during storm from 15 march to 20 march over arctic region. TEC data are plotted with time and latitude scale during the storm period, from the first panel showing the TEC fluctuation over Cambridge Bay, during the observation we notice the TEC is decreasing (<8TECU) during the storm time and after 24 hrsit's taking regular pattern, whole period of storm there is very less TEC observed. Second panel of figure showing Eureka station, there is also TEC activity is decreasing(>10 TECU) but little bit high as compare with Cambridge way we can see clearly in graph. Penal third is showing Rabbit Lake, there is TEC activity is high(>12 TECU) as compere to both stations.

Above segment we depicted exhaustively the perceptions. In this part, we will examine point by guide the outcomes all together toward decipher them. In Table 2, we have set up together the fundamental attributes of the tempest relying upon the longitudinal. There are a few actual systems for the arrangement of ionospheric anomalies in the polar ionosphere during TOI advancement, specifically Kelvin–Helmholtz and slope float insecurities (e.g., van der Meeren et al. 2014). Sojka et al. (1998) examined one such component. For the March 17, 2015 tempest, the two elements of the quick unbiased and plasma streams, affirmed by the Millstone Hill ISR estimations along with outdoors plasma upgrade (got from Swarm LP and outdoors GPS TEC estimations), support that ideal conditions for GDI advancement caused the event of the plasma thickness inconsistencies in the outdoors ionosphere. Expanded amplitudes of TEC varieties with expanding coupling rate probably mirror an expanded power of vivacious molecule precipitation, expanded thickness of polar patches comparative with the ionospheric foundation thickness, and, as a rule, a more unique and tempestuous polar cap with expanded magnetospheric convergence of sun oriented breeze energy. Biggest sufficiency TEC varieties were seen across early afternoon at scopes of 74.0–78.0° MLat. Huge postnoon amplitudes were noticed for lower coupling rates (<5000) and keeping in mind that prenoon and early afternoon amplitudes were biggest for higher coupling rates (>5000). These appropriations demonstrate expanded precipitation power in the postnoon area with expanded coupling rate and extraordinary precipitation around early afternoon and prenoon for high coupling rates >5000. Nilsson et al. [1998] noticed E district ionization because of particle precipitation at areas planning to the low scope cusp, in spite of the fact that it is hazy whether expanded coupling rates would strengthen this precipitation. The attractive field that interfaces the high-latitude ionosphere to the magnetosphere permits the immediate passage of particles of sunlight based breeze and magnetospheric beginning into the polar ionosphere during calm/upset occasions. The power of these cycles improves during times of toward the south interplanetary attractive field (IMF) which is an important condition for the magnetopause disintegration (Aubry et al., 1970; Meng, 1970). Dayside reconnection brings about the reallocation of attractive motion and fortifying of the magnetospheric convection electric fields and field-aligned flows, prompting polar cap development and equatorward development of the auroral oval (Le et al., 2016). The high-latitude ionosphere is likewise influenced by the attractive substorms (Elphinstone et al., 1996)

CONCLUSION

17 March 2015 was considerably bigger in size when contrasted with different tempests and shifted in accordance with the force of the geomagnetic storm. The St. Patrick's Day tempest of 2015 was an exceptionally upset period with solid coupling of the SWMI framework during the whole principle period of the tempest. The presence of improved plasma thickness in the TOI

shaped in the southern polar cap on 17 March 2015 is a consequence of the mind bogglingcoupling of the sunlight based wind-magnetosphere-ionosphere framework through electric fields and nonpartisan breezes for long lengths. The solid and supported magnetopause disintegration on 17 March 2015 prompted the pervasiveness of more grounded storm time electric fields beginning from the early principle period of the tempest. This examination shows that the length and degree of magnetopause disintegration assume a significant part in the spatiotemporal development of the plasma thickness dissemination in the high-multitude ionosphere. This investigation features the way that the conduct of the polar ionosphere is unequivocally affected by the outside drivers of geomagnetic storms and gives understanding into the idea of association of the sun oriented breeze with the earthly IT framework during the St. Patrick's Day of 2015. In this paper, ionospheric reactions to the geomagnetic storms on 17 March 2015 are explored by utilizing the GPS perceptions. Our principle discoveries are summed up as follows.

Total electron content fluctuation was very low observed over Cambridge Bay during storm time, 15 March to 20 March 2015 over arctic region and after 24 hrs it’s taking regular pattern. Over Eureka station, there is also TEC activity is decreasing but little bit high as compare with Cambridge way.For the Rabbit Lake station, there is TEC activity is high as compere to both stations during the storm period.

Disclaimer (Artificial intelligence)

Option 1:

Author(s) hereby declare that NO generative AI technologies such as Large Language Models (ChatGPT, COPILOT, etc) and text-to-image generators have been used during writing or editing of manuscripts.

Option 2:

Author(s) hereby declare that generative AI technologies such as Large Language Models, etc have been used during writing or editing of manuscripts. This explanation will include the name, version, model, and source of the generative AI technology and as well as all input prompts provided to the generative AI technology

Details of the AI usage are given below:

1.

2.

3.

Reference

Nie, W., Rovira-Garcia, A., Li, M., Fang, Z., Wang, Y., Zheng, D., & Xu, T. (2022). The mechanism for GNSS-based kinematic positioning degradation at high-latitudes under the March 2015 great storm. Space Weather, 20, e2022SW003132. https://doi. org/10.1029/2022SW003132

van der Meeren C, Oksavik K, Lorentzen D, Moen JI, Romano V (2014) GPS scintillation and irregularities at the front of an ionization tongue in the nightside polar ionosphere. J Geophys Res Space Phys 119:8624–8636. doi:10.1002/2014JA020114

Le, G., Luhr, H., Anderson, B. J., Strangeway, R. J., Russell, C. T., Singer, H., et al. (2016). Magnetopause erosion during the 17 March 2015magnetic storm: Combined field-aligned currents, auroral oval, and magnetopause observations. Geophysical Research Letters, 43,2396–2404. https://doi.org/10.1002/2016GL068257.

Jayachandran, P. T., K. Hosokawa, K. Shiokawa, Y. Otsuka, C. Watson, S. C. Mushini, J. W. MacDougall, P. Prikryl, R. Chadwick, and T. D. Kelly(2012), GPS total electron content variations associated with poleward moving Sun-aligned arcs, J. Geophys. Res., 117, A05310,doi:10.1029/2011JA017423.

Jayachandran, P. T., C. Watson, I. J. Rae, J. W. MacDougall, D. W. Danskin, R. Chadwick, T. D. Kelly, P. Prikryl, K. Meziane, and K. Shiokawa (2011),High-latitude GPS TEC changes associated with a sudden magnetospheric compression, Geophys. Res. Lett., 38, L23104,doi:10.1029/2011GL050041.

Aubry, M. P., Russel, C. T., &Kivelson, M. G. (1970). Inward motion of the magnetopause before a substorm. Journal of GeophysicalResearch, 75, 7018–7031. https://doi.org/10.1029/JA075i034p07018.

Buonsanto, M. J. (1999). Ionospheric storms-Review. Space Science Reviews, 88, 563–601.

Elphinstone, R. D., Murphree, J. S., & Cogger, L. L. (1996). What is a global auroral substorm? Reviews of Geophysics, 34, 169–232.

Gonzalez, W. D., Joselyn, J. A., Kamide, Y., Kroehl, H. W., Rostoker, G., Tsurutani, B. T., &Vasyliunas, V. M. (1994). What is a geomagneticstorm. Journal of Geophysical Research, 99(A4), 5771–5792.

Meng, C. I. (1970). Variation of the magnetopause position with substorm activity. Journal of Geophysical Research, 75, 3252.

Prölss, G. W. (1995). Ionospheric F-region storms. In H. Volland (Ed.), Handbook of atmospheric electrodynamics (Vol. 2, pp. 195–248).

Mendillo, M., 2006. Storms in the ionosphere: patterns and processes fortotal electron content. Rev. Geophys. 44, RG4001. https://doi.org/10.1029/2005RG000193.

Fuller-Rowell, T.J., Codrescu, M.V., Rishbeth, H., Moffett, R.J., Quegan,S., 1996. On the seasonal response of the thermosphere and ionosphereto geomagnetic storms. J. Geophys. Res. 101, 2343–2353.

Bilitza, D., and B. W. Reinisch (2008), International Reference Ionosphere 2007: Improvements and new parameters, Adv. Space Res., 42,599–609, doi:10.1016/j.asr.2007.07.048.

Jayachandran, P. T., et al. (2009), Canadian High Arctic Ionospheric Network (CHAIN), Radio Sci., 44, RS0A03, doi:10.1029/2008RS004046.

Nilsson, H., S. Kirkwood, and T. Moretto (1998), Incoherent scatter radar observations of the cusp acceleration region and cusp field-alignedcurrents, J. Geophys. Res., 103, 26,721–26,730, doi:10.1029/98JA02269.

Prikryl, P., P. T. Jayachandran, R. Chadwick, and T. D. Kelly (2015), Climatology of GPS phase scintillation at northern high latitudes for theperiod from 2008 to 2013, Ann. Geophys., 33, 531–545, doi:10.5194/angeo-33-531-2015.

Burns, A. G., T. L. Killeen, W. Deng, G. R. Carignan, and R. G. Roble (1995), Geomagnetic storm effects in the low-latitude to middle-latitudeupper thermosphere, J. Geophys. Res., 100, 14,673–14,691, doi:10.1029/94JA03232.

Richmond, A. D., and G. Lu (2000), Upper-atmospheric effects of magnetic storms: A brief tutorial, J. Atmos. Sol. Terr. Phys., 62, 1115–1127,doi:10.1016/S1364-6826(00)00094-8.

Prölss, G. W. (1995), Ionospheric F-region storms, in Handbook of Atmospheric Electrodynamics, edited by H. Volland, pp. 195–248 , CRC Press,Boca Raton, Fla.